Two-wavelength thermo-optical determination of Light Absorbing Carbon in atmospheric aerosols

Dario Massabò[1,*], Alessandro Altomari[2], Virginia Vernocchi[1], Paolo Prati[1]

1: Dept. of Physics, University of Genoa & INFN, Via Dodecaneso 33, 16146, Genova, Italy

2: Dept. of Physics, University of Genoa, Via Dodecaneso 33, 16146, Genova, Italy

Abstract

Thermo-optical analysis is widely adopted for the quantitative determination of Total, TC, Organic, OC, and Elemental, EC, Carbon in atmospheric aerosol sampled by suitable filters. Nevertheless, the methodology suffers of several uncertainties and artefacts as the well-known issue of charring affecting the OC-EC separation. In the standard approach, the effect of the possible presence of Brown Carbon, BrC, in the sample is neglected. BrC is a fraction of OC, usually produced by biomass burning with a thermic behaviour intermediate between OC and EC. BrC is optically active: it shows an increasing absorbance when the wavelength moves to the blue/UV region of the electromagnetic spectrum. Definitively, the thermo-optical characterization of carbonaceous aerosol should be reconsidered to address the possible BrC content in the sample under analysis.

We introduce here a modified Sunset Lab Inc. EC/OC Analyzer. Starting from a standard commercial instrument, the unit has been modified at the Physics Department of the University of Genoa (IT), making possible the alternative use of the standard laser diode at $\lambda = 635$ nm and of a new laser diode at $\lambda = 405$ nm. In this way, the optical transmittance through the sample can be monitored at both the wavelengths. Since at shorter wavelengths the BrC absorbance is higher, a better sensitivity to this species is gained. The modified instrument also gives the possibility to quantify the BrC concentration in the sample at both the wavelengths. The new unit has been thoroughly tested, with both artificial and real-world aerosol samples: the first experiment, in conjunction with the Multi Wavelength Absorbance Analyzer (MWAA, Massabò et al., 2013 and 2015), resulted in the first direct determination of the BrC Mass Absorption Coefficient (MAC) at $\lambda = 405$ nm: MAC = 23 ± 1 m^2 g^{-1}.

Keywords*: carbonaceous aerosol, brown carbon, thermo-optical analysis, mass absorption coefficient*

* Corresponding Author: massabo@ge.infn.it

1. Introduction

Light absorbing carbon (LAC) is the fraction of carbonaceous aerosol, which can absorb electromagnetic radiation in the visible or near-visible range (Pöschl, 2003; Bond and Bergstrom, 2006; Moosmüller et al., 2009; Ferrero et al., 2018). A wide literature investigates and characterizes the optical properties of the inorganic-refractory LAC fraction, usually referred as Black Carbon, BC, (e.g. Bond et al., 2013; and reference therein) which is strongly absorbing from UV to IR, with a weak dependence on wavelength (Bond and Bergstrom, 2006; Moosmüller et al., 2009). Much less studied and understood is the organic LAC, often labelled as Brown Carbon, which appears to be optically active at wavelengths shorter than 650 nm and with an increasing absorbance moving to the blue and ultraviolet (UV) range (Pöschl, 2003; Andreae and Gelencsér, 2006; Moosmüller et al., 2011; Laskin et al., 2015; Olson et al., 2015). BrC can therefore be considered as the "optically active" part of the OC dispersed in the atmosphere. When considered from a thermo-chemical point of view, BrC also shows a refractory behaviour since, in an inert atmosphere, it volatizes at temperatures greater than 400 °C only (Chow et al., 2015). A discussion on the primary and secondary sources of atmospheric LAC is outside the scope of the present work; we simply remind that primary BrC is produced mainly by biomass burning even if, in some cases, also incomplete combustion of fossil fuels used in transport activities (i.e. terrestrial vehicles, ships and aircrafts) can generate this kind of compounds (Corbin et al, 2018). It is also worth to underline that carbonaceous aerosols impact on human health (Pope and Dockery, 2006; Chow et al., 2006; Mauderly and Chow, 2008), as well as on climate and environment (Bond and Sun, 2005; Highwood and Kinnersley, 2006; Chow et. al., 2010).

In the wider landscape of atmospheric carbonaceous aerosol, despite a worldwide diffused effort, the situation is not satisfactory and a standardized and conclusive approach is still missing. The quantitative determination of TC, OC and EC is often performed by a thermo-optical analysis (Birch and Cary, 1996; Watson et al., 2005; Hitzenberger et al., 2006) of aerosol samples collected on quartz fibre filters. However, thermo-optical analyses are affected by several issues and artefacts (Yang and Yu, 2002; Chow et al., 2004) and different laboratories/agencies adopt protocols which systematically result in discrepancies, particularly large in the EC quantification (Birch and Cary, 1996; Chow et al., 2007; Cavalli et al., 2010). A further issue arises when the effects of the possible presence of BrC in the sample are taken into account. So far, the monitoring of the sample transmittance during the thermal cycle, has been introduced to correct for the well know charring effect and the formation of pyrolytic

carbon (Birch and Cary, 1996). This implies that BC is the sole absorbing compound at the wavelength implemented in the thermo-optical analyser (for instance at λ = 635 nm, the wavelength of the laser diode mounted in the extremely diffused Sunset Lab. Inc. EC/OC analyzer). Basically, with a sizeable concentration of BrC in the sample, one of the key assumptions of the thermo-optical methods fails and the EC/OC separation is even more unstable (to not say that, by design, the BrC quantification is not possible). This issue was preliminarily addressed by (Chen et al., 2015) by a multi-wavelength TOT/TOR instrument (Thermal Spectral Analysis – TSA) and further investigated in (Massabò et al., 2016). In the latter work, a method to correct the results of a standard Sunset analyzer and to retrieve the BrC concentration in the sample was introduced. The achievement was possible thanks to a synergy with the information provided by the Multi Wavelength Absorbance Analyzer, MWAA, (Massabò et al., 2015) developed in the same laboratory. A further step towards BrC quantification through the utilization of TSA was discussed in (Chow et al., 2018), where it was proved that the use of 7-wavelengths in thermal/optical carbon analysis allows contributions from biomass burning and secondary organic aerosols to be estimated. It is worthy to note that the biomass burning contribution to PM concentration can be also estimated by other methods such as Aerosol Mass Spectrometry, AMS (Daellenbach et al., 2016).

The MWAA approach allows the determination of the spectral dependence of the aerosol absorption coefficient (b_{abs}) which can be generally described by the power-law relationship $b_{abs}(\lambda) \sim \lambda^{-AAE}$, where the AAE is the Ångström Absorption Exponent. Several works reported AAE values which depend on the aerosol chemical composition (Kirchstetter et al., 2004; Utry et al., 2013) as well as its size and morphology (Lewis et al., 2008; Lack et al., 2012; Lack and Langridge, 2013; Filep et al., 2013; Utry et al., 2014). Furthermore, the spectral dependence of the aerosol has been exploited to identify different sources of carbonaceous aerosol (e.g. Sandradewi et al., 2008; Favez et al., 2010; Lack and Langridge, 2013; Massabò et al., 2013 and 2015). In general, AAE values close to 1.0 have been found to be related to urban PM where fossil fuels combustion is dominant, while higher AAE values, up to 2.5, have been linked to carbonaceous aerosols produced by wood burning (Harrison et al., 2013; and references therein) and therefore to the presence of BrC.

In the previous work by (Massabò et al., 2016) the effect of the BrC possibly contained in the sample on the thermo-optical analysis was quantified and exploited to retrieve the BrC concentration from the raw data provided by a standard Sunset Lab. Analyzer. This first step, suggested to modify/upgrade a Sunset unit adding the possibility to use a second laser diode in

the blue range. This improves the sensitivity to the BrC and allows to check whether the BrC quantification depends on the adopted wavelength. We finally followed this route and we here introduce our modified Sunset Analyzer unit, the validation tests and the results of the first campaign in which the new unit was deployed.

2. Materials and Methods

2.1 The 2-lambda SUNSET analyzer

We have modified a commercial Thermal Optical Transmittance (TOT) instrument (Sunset Lab Inc.). This equipment had been originally designed (Birch and Cary, 1996) with a red laser diode (λ = 635 nm) to have the possibility to monitor and correct the well know problem of the formation of pyrolytic carbon by charring (Birch and Cary, 1996; Bond and Bergstrom, 2006; Chow et al., 2007; Cavalli et al., 2010). The assumption that OC is optically inactive at wavelengths greater than 600 nm is at the basis of the technique; therefore the laser beam attenuation is only due to the EC originally present or formed by charring in the sample under analysis. Actually, even at this wavelength, BrC can affect the reliability of the OC/EC separation and the standard methodology can be modified to quantify the BrC concentration (Massabò et al., 2016). Nevertheless, at λ = 635 nm the BrC Mass Absorption Coefficient, MAC(BrC), remains much smaller of the corresponding MAC(BC) and the modified procedure could/should be implemented at shorter wavelengths to gain in sensitivity.

We have modified our SUNSET unit making possible the alternative use of the standard laser diode at λ = 635 nm or of a World Star Technologies, 100 mW, laser diode at λ = 405 nm. This second laser diode can be mounted on the top of the SUNSET furnace by a homemade adapter (see Figure 1) and easily exchanged with the native red diode. With the new laser diode, the light detector placed at the bottom of the SUNSET furnace has to be changed too and we selected a photodiode (PD) THORLABS FDS1010 coupled with a bandpass filter THORLABS FBH405-10. The responsivity of the PD FDS1010 around λ = 400 nm is quite low (about 50 mA W^{-1}) but the high power delivered by the laser diode results in signals with an amplitude comparable to the values measured with the original SUNSET set-up (i.e. laser diode and PD). Furthermore, the FBH405-10 filter cuts all the light background produced by the high temperature of the SUNSET furnace, thus preserving the signal-to-noise ratio. Both laser and PD can be exchanged in about 10 min and no particular attention is requested but the proper alignment to maximize the PD output signal (i.e. the *transmittance* value displayed by

the SUNSET control software). We have to note that the original configuration of the SUNSET instrument adopts a lock-in amplifier to improve the signal-to-noise ratio of the PD: we did not have the possibility to manipulate the parameters of the lock-in amplifier and to tune it to the new configuration.

2.2 Test of the new configuration

The new blue-light set-up of the Sunset Analyzer was tested using both synthetic and real-world aerosol samples, collected on quartz fibre filters. Synthetic samples were prepared starting with a 5% (volume) solution of Aquadag, then nebulised by a Blaustein Atomizer (BLAM) and collected on quartz fibre filters. Aquadag is the trade name of a water-based colloidal graphite coating (particle diameters between 50 and 100 nm): these samples can therefore be considered to be composed by EC/BC only. The samples were first sent to an optical characterization by the MWAA instrument (Multi Wavelength Absorbance Analyzer, Massabò et al., 2015) which demonstrated that the optical absorption of Aquadag is independent on the wavelength. Actually, Aquadag particles tend to form conglomerates on the filter surface, with dimension about double of the longer wavelength implemented in the MWAA (i.e. the 850 nm of the infrared laser diode; Massabò et al., 2015). So, the comparison between the two Sunset set-ups was made with samples having the same absorption properties. EC and TC quantifications obtained at $\lambda = 635$ nm and $\lambda = 405$ nm resulted compatible adopting both the NIOSH5040 and EUSAAR_2 protocol (Cavalli et al., 2010), as shown in Figure 2 for the whole set of synthetic samples.

A second set of synthetic samples was prepared to mimic the behaviour of real-world aerosol samples: a 3% (weight) solution of ammonium sulphate $(NH_4)_2SO_4$ in Aquadag was prepared and nebulized with the BLAM. This way, a scattering compound is mixed to the absorbing Aquadag spherules. The optical absorption measured with MWAA resulted independent on wavelength with this second set of samples too. The results of the Sunset analysis with both the red and blue laser set-up are shown in Figure 3. This second set of samples was analysed through the EUSAAR_2 protocol only: we used two punches for each laser in each sample to have a reproducibility check. A strong correlation between the TC and EC values measured in red and blue light was obtained again with a slope close to unity.

A third and final test was performed using a set of daily PM10 samples collected by a low-volume sampler (TCR - Tecora, Italy) on quartz fibre filters (Pall-2500 QAO-UP, 47 mm diameter) in spring 2016 in the urban area of the city of Genoa (IT). A previous and long set of similar campaigns addressed to PM10 characterization (e.g. Bove et al., 2014 and references

therein) in the same urban area could not identify sizeable contributes of biomass burning to PM composition, in particular during spring and summer. Such situation was confirmed by the determination of the Ångström exponent in the present samples by the MWAA. Actually, in the set of twenty PM10 samples, the values of the Ångström exponent ranged between 0.9 and 1.2, this confirming that Black Carbon is the sole or totally dominant light absorbing component in the local PM10 (Sandradewi et al., 2008; Harrison et al., 2013). Half of the samples was then sent to the Sunset analysis by the NIOSH5040 protocol while the EUSAAR_2 protocol was adopted for the remaining subset. The results are shown in Figure 4. The EC concentration values measured with the standard and modified Sunset analyzer are fully compatible when the NIOSH5040 protocol is adopted (basically, the split point position in the Sunset thermogram does not change with the two laser diodes). Instead, EC values determined by the EUSAAR_2 protocol resulted lower by about 30% when the blue laser diode was mounted. This corresponds to a shift of the split point position, which moves rightward and thus increases the amount of carbonaceous aerosol counted in the OC fraction. This effect is linked to the well-known issue of the formation of pyrolytic carbon during the thermal cycle in the inert atmosphere (i.e. in He). Several literature studies (e.g.: Cavalli et al., 2010; Panteliadis et al., 2015) indicated that the charring is smaller at the higher temperatures reached during the NIOSH thermal protocol. On the other way, standard thermo-optical analyses of urban PM samples often give higher EC values (up to 50%) when performed following the EUSAAR_2 instead of higher-temperature protocols (Subramanian et al., 2006; Zhi et al., 2008; Piazzalunga et al., 2011; Karanasiou et al., 2015; Panteliadis et al., 2015). Furthermore, as by-product of previous PM10 studies in the urban area of Genoa by a standard Sunset unit, we could observe a systematic and very reproducible 40% discrepancy between EC values determined in the same samples by EUSAAR_2 and NIOSH5040 protocols (with EC:EUSAAR > EC:NIOSH). Therefore, the thermo-optical analysis in blue light seems to be more sensitive to the charring formation during the EUSAAR_2 protocol and thus possibly more reliable in the EC/OC separation.

3. First field campaign and results

The modified Sunset instrument was used for the first time, in conjunction with the MWAA instrument and apportionment methodology (Massabò et al., 2015), to retrieve the MAC (Mass Absorption Coefficient) of Brown Carbon at the two wavelengths of $\lambda = 635$ nm and $\lambda = 405$ nm, in a set of samples collected wintertime in a mountain site.

205

206 ***3.1 Samples collection***

207 Aerosol samples were collected in a small village (Propata, 44°33'52.93''N, 9°11'05.57''E,
208 970 m a.s.l.) situated in the Ligurian Apennines, Italy. Three different sets of PM10 aerosol
209 samples were collected by a low-volume sampler (38.3 l min^{-1} by TCR Tecora): the first and
210 the third sets had filter change set every 24h while the second set was sampled on a 48h-basis.
211 In total, 41 (14+13+14) PM10 samples were collected on quartz-fibre filters (Pall, 2500QAO-
212 UP, 47 mm diameter), between February 2nd and April 19th, 2018. Before the sampling, the
213 filters were baked at T = 700°C for 2 hours to remove possible internal contamination. Field
214 blank filters were used to monitor possible contaminations during the sampling phase. Wood
215 burning is one of the PM sources around the sampling site, especially during the cold season,
216 as it is used for both domestic heating and cooking purposes.

217

218 ***3.2 Laboratory analyses***

219 All the samples were weighed before and after sampling in an air-conditioned room (T = 20
220 ± 1 °C; R.H. = 50 % ± 5%), after 48h conditioning. The gravimetric determination of the PM
221 mass was performed using an analytical microbalance (precision: 1 μg) which was operated
222 inside the conditioned room; electrostatic effects were avoided by the use of a de-ionizing gun.

223 After weighing, samples were first optically analyzed by MWAA to retrieve the absorption
224 coefficient (b_{abs}) of PM at five different wavelengths. The EC and OC determination was
225 performed adopting the EUSAAR_2 protocol (Cavalli et al., 2010) with both laser diodes at λ
226 = 635 nm and at λ = 405 nm (two different punches were extracted from each filter sample).

227 Finally, the remaining portion of the same quartz-fibre filters underwent a chemical
228 determination of the Levoglucosan (1,6-Anhydro-beta-glucopyranose) concentration by High
229 Performance Anion Exchange Chromatography coupled with Pulsed Amperometric Detection
230 (Piazzalunga et al., 2010). As well known in literature, this sugar is one of the typical marker
231 of biomass burning (Vassura et al., 2014).

232

233 ***3.3 Optical apportionment***

234 The MWAA analysis provided the raw data to measure the spectral dependence of the
235 aerosol absorption coefficient (b_{abs}) which can be generally described by the power-law
236 relationship $b_{abs}(\lambda) \sim \lambda^{-AAE}$ where AAE is the Ångström Absorption Exponent.

The time series of the resulting AAE values is shown in Figure 5: they range between 1.05 and 1.96 with a mean value of 1.55 ± 0.21. This figure indicates a substantial presence of wood burning in the sampling area. In (Massabò et al., 2015 and Bernardoni et al, 2017), an optical apportionment model (the "MWAA model") based on the measurement of b_{abs} at five wavelengths had been introduced to obtain directly the BrC AAE (α_{BrC}) and the BrC absorption coefficient (b_{abs}^{BrC}) at each measured wavelength. It is worthy to note that, at the basis of the MWAA model, there is the assumption that BrC is produced by wood combustion only (see §4 in Massabò et al., 2015; Zheng et al., 2013). In Figure 5, we report the optical apportionment at λ = 635 nm and at λ = 405 nm i.e. at the wavelength of the two laser diodes used in our modified Sunset instrument. At λ = 635 nm, light absorption resulted mainly due to BC from both fossil fuel (FF) and wood burning (WB) and the b_{abs}^{BrC} average value is 15% of total b_{abs}, with the notable exception of some days in which it reached values of ~ 30%, in correspondence of AAE > 1.9. Instead, at λ = 405 nm, the BrC contribute to light absorption rises up to 33% (average percentage of total b_{abs}), with a maximum value of 51%, again when AAE_{exp} > 1.9. The time series of b_{abs}^{BrC} values at both the wavelengths turned out to be well correlated (R^2 = 0.71) with the Levoglucosan (*Levo*, in the following) concentration values, as reported in Figure 6. The slope of the correlation curve increases by a factor 5.8 when moving from the red to the blue light.

The average α_{BrC} value turned out to be α_{BrC} = 3.9 ± 0.1, in very good agreement with a previous value (α_{BrC} = 3.8 ± 0.2) obtained in the same site and with the same approach (Massabò et al., 2016). The result is also in agreement with other literature works (Yang et al., 2009; Massabò et al., 2015; Chen et al., 2015).

3.4 Brown Carbon MAC

The methodology to extract the MAC value for BrC by the coupled used of MWAA and Thermo-Optical Analysis has been introduced in a previous work (Massabò et al., 2016). In that case, a standard (i.e.: with a red laser diode only) Sunset unit was used. The entire procedure is described in details in (Massabò et al., 2016), here we briefly summarize the main steps:

a) The fraction of light attenuation due to the BrC is first calculated in each sample with the MWAA raw data.
b) The empirical relationship between the light attenuation through the sample, observed in the MWAA and in the Sunset and at both wavelengths, is then determined. We remind

that in the Sunset measurement, the light attenuation is continuously recorded during the analysis; the value characteristic of each blank filter can be retrieved when all the light absorbing PM has been volatized (i.e. at the end of the thermal protocol).

c) The fraction of light attenuation due to the BrC in the sample is therefore calculated for the Sunset analysis and the initial transmittance value is corrected to estimate the attenuation value that it would have been found if BrC were not present in the filter sample.

d) A new split-point position is then determined taking into account the corrected value of the initial transmittance.

e) The OC and EC values determined with the standard and corrected split-point positions are then compared and the difference ($OC_{cor} - OC_{std} = EC_{std} - EC_{cor}$) is operatively assumed to be equal to the BrC in the sample. The corresponding BrC atmospheric concentration is finally calculated.

f) The correlation between the values of b_{abs}^{BrC}, provided by the MWAA analysis (see section 3.3) and BrC concentration, is studied to determine the MAC value.

In the present experiment, the procedure was adopted to analyse the thermograms produced with both the red and the blue laser diode mounted in the Sunset unit: the results are summarized in Figure 7. Despite a rather high noise in the data, the MAC(BrC) value at the two wavelengths can be determined and it turns out to be MAC(BrC) = 9.8 ± 0.4 $m^2 g^{-1}$ and 23 ± 1 $m^2 g^{-1}$, respectively at λ = 635 and 405 nm. This result deserves some comments:

- The MAC value at λ = 635 nm differs for about 3σ from the result reported in (Massabò et al., 2016) and obtained in the same site and in a similar season (i.e. November 2015 to January 2016; MAC = 7.0 ± 0.4 $m^2 g^{-1}$). Since differences in the type of wood burnt in the past and present campaign cannot be excluded, the two values can be considered to be in fair agreement.
- No comparison with previous or other literature values is possible for the MAC value at λ = 405 nm, given the substantial differences in adopted definitions and methodologies (Yang et al., 2009; Feng et al., 2013; Chen and Bond, 2010). However, the increase by a factor 2.3 with respect to the MAC at λ = 635 nm follows the expected behaviour.
- Under the assumption that the sole source of BrC is biomass burning, the MAC values can be referred to the total concentration of organic carbon (i.e. including the part not

optically active) produced by biomass burning. Adopting with the present data set the optical OC apportionment methodology reported in (Massabò et al., 2015), the BrC values determined at $\lambda = 635$ nm turn out to be about 4% of the OC produced by wood combustion, OC_{WB}, and consequently MAC($OC_{WB,}$ $\lambda = 635$nm) = 0.39 ± 0.06 m^2 g^{-1}. When the analysis is performed at $\lambda = 405$ nm, BrC results to be about 10% of OC_{WB} and MAC($OC_{WB,}$ $\lambda = 405$nm) = 2.3 ± 0.2 m^2 g^{-1}. Previous literature works (Feng et al., 2013; Laskin et al., 2015; and references therein) report MAC values of BrC and/or related OC ranging in a quite large interval.

- The ratio between BrC and Levo concentration values results to be BrC:Levo = 0.19 ± 0.02 and 0.42 ± 0.06, respectively when considering the BrC concentration determined by MWAA + Sunset at $\lambda = 635$ and 405 nm. In other words, the operative procedure, introduced in (Massabò et al., 2016), results in different BrC concentration values according to the considered/used wavelength. This fact can be interpreted in different ways: while the analytical sensitivity is higher at $\lambda = 405$ nm and the corresponding BrC values could be considered to be more firm, the category of compounds collected under the label "Brown Carbon" could be itself "wavelength dependent". The latter would imply that the BrC concentration cannot be defined separately from the wavelength and that its meaning is even more "operative" of the more widespread OC and EC fractions. As a matter of fact, while the b_{abs}^{BrC} values discussed in section 3.3, increase by a factor 5.8 moving from $\lambda = 635$ nm to $\lambda = 405$ nm, the corresponding variation of the MAC(BrC) values is by a factor 2.3 only. This is because the BrC concentration determined at $\lambda = 405$ nm doubles the value measured at $\lambda = 635$ nm. The purposes and the limits of the present study prevent any firm conclusion on the alternative explanation: BrC definition is wavelength dependent or the analysis in red light is not sensitive enough.
- When considering the OC_{WB}:Levo concentration ratio, the MWAA analysis at $\lambda = 635$ and $\lambda = 405$ nm give well compatible results, with a mean value of OC_{WB}:Levo = 4.5 ± 0.5.

4. Conclusions

We introduced a modified version of a commercial Sunset Lab. Inc. OC/EC Analyzer. We upgraded the standard instrument unit making possible the alternative use of a red ($\lambda = 635$

nm) or blue (λ= 405 nm) laser diode to monitor the light transmittance through the sample during the thermal cycle. The analytical performance of the new set-up has been tested both with artificial and real-world aerosol samples.

The new Sunset set-up was used to analyze a set of samples collected mostly wintertime in a mountain site of the Italian Apennines. We retrieved Brown Carbon concentration values directly from the Sunset thermograms following Massabò et al., 2016. Exploiting the synergic information provided by the Multi Wavelength Absorbance Analyzer, MWAA (Massabò et al., 2015) we could obtain the MAC(BrC) at the two wavelengths. The result at λ = 635 nm (MAC = 9.8 ± 0.4 m^2 g^{-1}) is in fair agreement with a previous study performed in the same site in winter 2015-2016. At our knowledge, the result at λ = 405 nm, MAC = 23 ± 1 m^2 g^{-1} is the sole direct observation at this wavelength.

In our findings, the ratio between BrC and Levo concentration values depends on the wavelength of the transmittance signal adopted during the thermo-optical analysis. This behaviour could be due to 1) a better accuracy of the results in blue-light, more sensitive to BrC, or 2) the definition of BrC itself, which has to be considered wavelength-dependent. The present results do not allow any conclusive statement on this issue: actually, the label "Brown Carbon", as well as the widely used "Organic and Elemental Carbon", comes from an operative definition not without ambiguity.

6. Acknowledgements

This work has been partially financed by the National Institute of Nuclear Physics (INFN) in the frame of the TRACCIA experiments.

References

Andreae, M. O. and Gelencsér, A.: Black Carbon or Brown Carbon? The nature of light-absorbing carbonaceous aerosol, Atmos. Chem. Phys., 6, 3131-3148, 2006.

Bernardoni, V., Pileci, R. E., Caponi, L., and Massabò, D.: The Multi-Wavelength Absorption Analyzer (MWAA) model as a tool for source and component apportionment based on aerosol absorption properties: application to samples collected in different environments, Atmosphere, 8, 218, 2017.

Birch, M. E. and Cary, R. A.: Elemental carbon-based method for occupational monitoring of particulate diesel exhaust: methodology and exposure issues, Analyst, 121, 1183–1190, 1996.

Bond, T. C. and Bergstrom, R. W.: Light absorption by carbonaceous particles: an investigative review, Aerosol Sci. Tech., 40, 27-67, 2006.

Bond, T. C. and Sun, H. L.: Can reducing black carbon emissions counteract global warming?, Environ. Sci. Technol., 39, 5921–5926, 2005.

Bond, T. C., Doherty, S. J., Fahey, D. W., Forster, P. M., Berntsen, T., De Angelo, B. J., Flanner, M. G., Ghan, S., Kärcher, B., Koch, D., Kinne, S., Kondo, Y., Quinn, P. K., Sarofim, M. C., Schultz, M. G., Schulz, M., Venkataraman, C., Zhang, H., Zhang, S., Bellouin, N., Guttikunda, S. K., Hopke, P. K., Jacobson, M. Z., Kaiser, J. W., Klimont, Z., Lohmann, U., Schwarz, J. P., Shindell, D., Storelvmo, T., Warren, S. G., and Zender, C. S.: Bounding the role of black carbon in the climate system: a scientific assessment, J. Geophys. Res.-Atmos., 118, 5380-5552, 2013.

Bove, M. C., Brotto, P., Cassola, F., Cuccia, E., Massabò, D., Mazzino, A., Piazzalunga, A., and Prati, P.: An integrated PM2.5 source apportionment study: positive matrix factorisation vs. the chemical transport model CAMx, Atmos. Environ., 94, 274-286, 2014.

Cavalli, F., Putaud, J. P., Viana, M., Yttri, K. E., and Gemberg, J.: Toward a standardized thermal-optical protocol for measuring atmospheric Organic and Elemental Carbon: the EUSAAR protocol, Atmos. Meas. Tech., 3, 79-89, 2010.

Chen, Y. and Bond, T. C.: Light absorption by organic carbon from wood combustion, Atmos. Chem. Phys., 10, 1773–1787, 2010.

Chen, L. W. A., Chow, J. C., Wang, X. L., Robles, J. A., Sumlin, B. J., Lowenthal, D. H., Zimmermann, R., and Watson, J. G.: Multi-wavelength optical measurement to enhance thermal/optical analysis for carbonaceous aerosol, Atmos. Meas. Tech., 8, 451-461, 2015.

Chow, J. C., Watson, J. G., Chen, L. W. A., Arnott, W. P., Moosmüller, H., and Fung, K. K.: Equivalence of elemental carbon by thermal/optical reflectance and transmittance with different temperature protocols, Environ. Sci. Technol., 38, 4414-4422, 2004.

Chow, J. C., Watson, J. G., Mauderly, J. L., Costa, D. L., Wyzga, R. E., Vedal, S., Hidy, G. M., Altshuler, S. L., Marrack, D., Heuss, J. M., Wolff, G. T., Pope, C. A. III, and Dockery, D. W.: Health effects of fine particulate air pollution: lines that connect, J. Air Waste Manag. Assoc., 56, 1368–1380, 2006.

Chow, J. C., Watson, J. G., Chen, L. W. A., Chang, M. C. O., Robinson, N. F., Trimble, D. L., and Kohl, S. D.: The IMPROVE_A temperature protocol for thermal/optical carbon analysis:

maintaining consistency with a long-term database, J. Air Waste Manag. Assoc., 57, 1014-1023, 2007.

Chow, J. C., Watson, J. G., Lowenthal, D. H., Chen, L. W. A., and Motallebi, N.: Black and organic carbon emission inventories: review and application to California, J. Air Waste Manag. Assoc., 60, 497–507, 2010.

Chow, J. C., Wang, X., Sumlin, B. J., Gronstal, S. B., Chen, L. W. A., Trimble, D. L., Kohl, S. D., Mayorga, S. R., Riggio, G., Hurbain, P. R., Johnson, M., Zimmermann, R., and Watson, J. G.: Optical calibration and equivalence of a multiwavelength thermal/optical carbon analyzer, Aerosol Air Qual. Res., 15, 1145-1159, 2015.

Chow, J.C, Watson, J. G., Green, M. C., Wang, X., Chen, L. W. A., Trimble, D. L., Cropper, P. M., Kohl S. D., and Gronstal, S. B.: Separation of brown carbon from black carbon for IMPROVE and Chemical Speciation Network PM2.5 samples, J. Air Waste Manag. Assoc., 68:5, 494-510, 2018.

Corbin J. C., Pieber S. M., Czech H., Zanatta M., Jakobi G., Massabò D., Orasche J., El Haddad I., Mensah A. A., Stengel B., Drinovec L., Mocnik G., Zimmermann R., Prévôt A. S. H., and M. Gysel: Brown and Black Carbon emitted by a marine engine operated on heavy fuel oil and distillate fuels: optical properties, size distributions, and emission factors, J. Geophys. Res-Atmos, 123, 6175–6195, 2018.

Daellenbach, K.R., Bozzetti, C., Křepelová, A., Canonaco, F., Wolf, R., Zotter, P., Fermo, P., Crippa, M., Slowik, J.G., Sosedova, Y., Zhang, Y., Huang, R. J., Poulain, L., Szidat, S., Baltensperger, U., El Haddad, I., and Prévôt, A. S. H.: Characterization and source apportionment of organic aerosol using offline aerosol mass spectrometry, Atmos. Meas. Tech., 9 (1), 23-39, 2016.

Favez, O., El Haddad, I., Piot, C., Boreave, A., Abidi, E., Marchand, N., Jaffrezo, J. L., Besombes, J. L., Personnaz, M. B., Sciare, J., Wortham, H., Geroge, C., and D'Anna, B.: Inter-comparison of source apportionment models for the estimation of wood burning aerosols during wintertime in an Alpine city (Grenoble, France), Atmos. Chem. Phys., 10, 5295-5314, 2010.

Feng, Y., Ramanathan, V., and Kotamarthi, V. R.: Brown carbon: a significant atmospheric absorber of solar radiation?, Atmos. Chem. Phys., 13, 8607-8621, 2013.

Ferrero, L., Močnik, G., Cogliati, S., Gregorič, A., Colombo, R., and Bolzacchini, E.: Heating rate of light absorbing aerosols: time-resolved measurements, the role of clouds, and source identification, Environ. Sci. Tech., 52 (6), 3546-3555, 2018.

Filep, Á., Ajtai, T., Utry, N., Pintér, M. D., Nyilas, T., Takács, S., Máté, Z., Gelencsér, A., Hoffer, A., Schnaiter, M., Bozóki, Z., and Szabó, G.: Absorption spectrum of ambient aerosol and its correlation with size distribution in specific atmospheric conditions after a red mud accident, Aerosol Air Qual. Res., 13, 49-59, 2013.

Harrison, R. M., Beddows, D. C. S., Jones A. M., Calvo A., Alves C., and Pio C.: An evaluation of some issues regarding the use of aethalometers to measure woodsmoke concentrations, Atmos. Environ., 80, 540-548, 2013.

Highwood, E. J. and Kinnersley, R. P.: When smoke gets in our eyes: the multiple impacts of atmospheric black carbon on climate, air quality and health, Environ. Int., 32, 560–566, 2006.

Hitzenberger, R., Petzold, A., Bauer, H., Ctyroky, P., Pouresmaeil, P., Laskus, L., and Puxbaum, H.: Intercomparison of thermal and optical measurement methods for elemental carbon and black carbon at an urban location, Environ. Sci. Technol., 40 (20), 6377-6383, 2006.

Karanasiou, A., Minguillon, M. C., Viana, M., Alaustey, A., Puaud, J. P., Maenhaut, W., Panteliadis, P., Močnik, G., Favez, O., and Kuhlbusch, T. A.: Thermal-optical analysis for the measurement of elemental carbon (EC) and organic carbon (OC) in ambient air, a literature review, Atmos. Meas. Tech. Discuss., 8, 9649-9712, 2015.

Kirchstetter, T. W., Novakok, T., and Hobbs, P. V.: Evidence that the spectral dependence of light absorption by aerosols is affected by organic carbon, J. Geophys. Res., 109, D21208, 2004.

Lack, D. A., Langridge, J. M., Bahreini, R., Cappa, C. D., Middlebrook, A. M., and Schwarz, J. P.: Brown carbon and internal mixing in biomass burning particles, Proc. Natl. Acad. Sci., 109, 14802-14807, 2012.

Lack, D. A. and Langridge, J. M.: On the attribution of black and brown carbon light absorption using the Ångström exponent, Atmos. Chem. Phys., 13, 10535-10543, 2013.

Laskin, A., Laskin, J., and Nizkorodov S. A.: Chemistry of atmospheric brown carbon, Chem. Rev., 115 (10), 4335–4382, 2015.

Lewis, K., Arnott, W. P., Moosmüller, H., and Wold, C. E.: Strong spectral variation of biomass smoke light absorption and single scattering albedo observed with a novel dual-wavelength photoacoustic instrument, J. Geophys. Res., 113, D16203, 2008.

Massabò, D., Bernardoni, V., Bove, M. C., Brunengo, A., Cuccia, E., Piazzalunga, A., Prati, P., Valli, G., and Vecchi, R.: A multi-wavelength optical set-up for the characterization of carbonaceous particulate matter, J. Aerosol Sci., 60, 34-46, 2013.

Massabò, D., Caponi, L., Bernardoni, V., Bove, M. C., Brotto, P., Calzolai, G., Cassola, F., Chiari, M., Fedi, M. E., Fermo, P., Giannoni, M., Lucarelli, F., Nava, S., Piazzalunga, A., Valli, G., Vecchi, R., and Prati, P.: Multi-wavelength optical determination of black and brown carbon in atmospheric aerosols, Atmos. Environ., 108, 1-12, 2015.

Massabò, D., Caponi, L., Bove, M. C., and Prati, P.: Brown carbon and thermal-optical analysis: a correction based on optical multi-wavelength apportionment of atmospheric aerosols, Atmos. Environ., 125, 119-125, 2016.

Mauderly, J. L. and Chow, J. C.: Health effects of organic aerosols, Inhal. Toxicol., 20, 257–288, 2008.

Moosmüller, H., Chakrabarty, R. K., and Arnott, W. P.: Aerosol light absorption and its measurement: a review, J. Quant. Spectrosc. Ra., 110, 844-878, 2009.

Moosmüller, H., Chakrabarty, R. K., Ehlers, K. M., and Arnott, W. P.: Absorption Ångström coefficient, brown carbon, and aerosols: basic concepts, bulk matter, and spherical particles, Atmos. Chem. Phys., 11, 1217-1225, 2011.

Olson, M. R., Garcia, M. V., Robinson, M. A., Van Rooy, P., Dietenberger, M. A., Bergin, M., and Schauer, J. J.: Investigation of black and brown carbon multiple-wavelength-dependent light absorption from biomass and fossil fuel combustion source emissions, J. Geophys. Res. Atmos., 120, 2015.

Panteliadis, P., Hafkenscheid, T., Cary, B., Diapouli, E., Fischer, A., Favez, O., Quincey, P., Viana, M., Hitzenberger, R., Vecchi, R., Saraga, D., Sciare, J., Jaffrezo, J. L., John, A., Schwarz, J., Giannoni, M., Novak, J., Karanasiou, A., Fermo, P., and Maenhaut, W.: ECOC comparison exercise with identical thermal protocols after temperature offset correction – instrument diagnostics by in-depth evaluation of operational parameters, Atmos. Meas. Tech., 8, 779–792, 2015.

Piazzalunga, A., Fermo, P., Bernardoni, V., Vecchi, R., Valli, G., and De Gregorio M. A.: A simplified method for levoglucosan quantification in wintertime atmospheric particulate matter by high performance anion-exchange chromatography coupled with pulsed amperometric detection, Int. J. Environ. An. Ch., 90, 934-947, 2010.

Piazzalunga, P., Bernardoni, V., Fermo, P., Valli, G., and Vecchi, R.: On the effect of water-soluble compounds removal on EC quantification by TOT analysis in urban aerosol samples, Atmos. Chem. Phys., 11, 10193-10203, 2011.

Pope, C. A. III and Dockery, D. W.: Health effects of fine particulate air pollution: lines that connect, J. Air Waste Manag. Assoc., 56, 709–742, 2006.

Pöschl, U.: Aerosol particle analysis: challenges and progress, Anal. Bioanal. Chem., 375, 3032, 2003.

Sandradewi, J., Prevot, A. H., Szidat, S., Perron, N., Rami Alfarra, M., Lanz, V., Weingartner, E., and Baltensperger, U.: Using aerosol light absorption measurements for the quantitative determination of wood burning and traffic emission contributions to particulate matter, Environ. Sci. Technol., 3316-3323, 2008.

Subramanian, R., Khlystov, A. Y., and Robinson, A. L.: Effect of peak inert-mode temperature on elemental carbon measured using thermal-optical analysis, Aerosol Sci. Tech., 40, 763–780, 2006.

Utry, N., Ajtai, T., Filep, Á., Dániel P. M., Hoffer, A., Bozoki, Z., and Szabó, G.: Mass specific optical absorption coefficient of HULIS aerosol measured by a four-wavelength photoacoustic spectrometer at NIR, VIS and UV wavelengths, Atmos. Environ., 69, 321-324, 2013.

Utry, N., Ajtai, T., Filep, Á., Pintér, M., Török, Zs., Bozóki, Z., and Szabó, G.: Correlations between absorption Angström exponent (AAE) of wintertime ambient urban aerosol and its physical and chemical properties, Atmos. Environ., 91, 52-59, 2014.

Vassura, I., Venturini, E., Marchetti, S., Piazzalunga, A., Bernardi, E., Fermo, P., and Passarini, F.: Markers and influence of open biomass burning on atmospheric particulate size and composition during a major bonfire event, Atmos. Environ., 82, pp. 218-225, 2014.

Watson, J. G., Chow, J. C., and Chen, L. W. A.: Summary of organic and elemental carbon/black carbon analysis methods and intercomparisons, Aerosol Air Qual. Res., 5, 65-102, 2005.

Yang, H. and Yu, J. Z.: Uncertainties in charring correction in the analysis of elemental and organic carbon in atmospheric particles by thermal/optical methods, Environ. Sci. Technol., 36, 5199-5204, 2002.

Yang, M., Howell, S. G., Zhuang, J., and Huebert, B. J.: Attribution of aerosol light absorption to black carbon, brown carbon, and dust in China - interpretations of atmospheric measurements during EAST-AIRE, Atmos. Chem. Phys., 9, 2035-2050, 2009.

Zheng, G., He, K., Duan, F., Cheng, Y., and Ma, Y.: Measurement of humic-like substances in aerosols: A review, Environ. Pollut., 181, 301-314, 2013.

Zhi, G., Chen, Y., Sheng, G., and Fu, J.: Effects of temperature parameters on thermal-optical analysis of organic and elemental carbon in aerosol, Environ. Monit. Assess., 154, 253–261, 2008.

FIGURE CAPTIONS

Figure 1: The new λ = 405 nm laser diode mounted by a steel adapter on the SUNSET furnace (top) and the comparison with the standard λ = 635 nm laser diode implemented by the manufacturer (bottom).

Figure 2: Quantification of TC (primary axis) and EC (secondary axis) at λ = 635 nm (red) and λ = 405 nm (blue) for the set of synthetic Aquadag samples. Top: NIOSH5040 protocol, bottom: EUSAAR_2 protocol.

Figure 3: Quantification of TC (primary axis) and EC (secondary axis) at λ = 635 nm (red) and λ = 405 nm (blue) for the set of synthetic Aquadag + Ammonium Sulphate samples by the EUSAAR_2 protocol.

Figure 4: EC concentration measured in two sub-sets of PM10 samples collected in consecutive days in the urban area of Genoa in late spring 2016. Values determined with the Sunset analyzer equipped with blue and red laser diodes, are compared.

Figure 5: Primary axis: Optical apportionment of the aerosol absorption coefficient (b_{abs}) at λ = 635 nm (top) and λ = 405 nm (bottom). Secondary axis: experimental AAE values obtained by fitting the measured b_{abs} values with a power-law relationship $b_{abs}(\lambda) \sim \lambda^{-AAE}$. FF and WB stand for Fossil Fuel and Wood Burning, respectively.

Figure 6: Aerosol absorption coefficient apportioned to Brown Carbon (b_{abs}^{BrC}) at λ = 635 nm (top) and at λ = 405 nm (bottom) vs. levoglucosan concentration.

Figure 7: Comparison between the aerosol absorption coefficient apportioned to Brown Carbon vs. the resulting operative BrC concentration values at λ = 635 nm (top) and at λ = 405 nm (bottom).

Figure 1

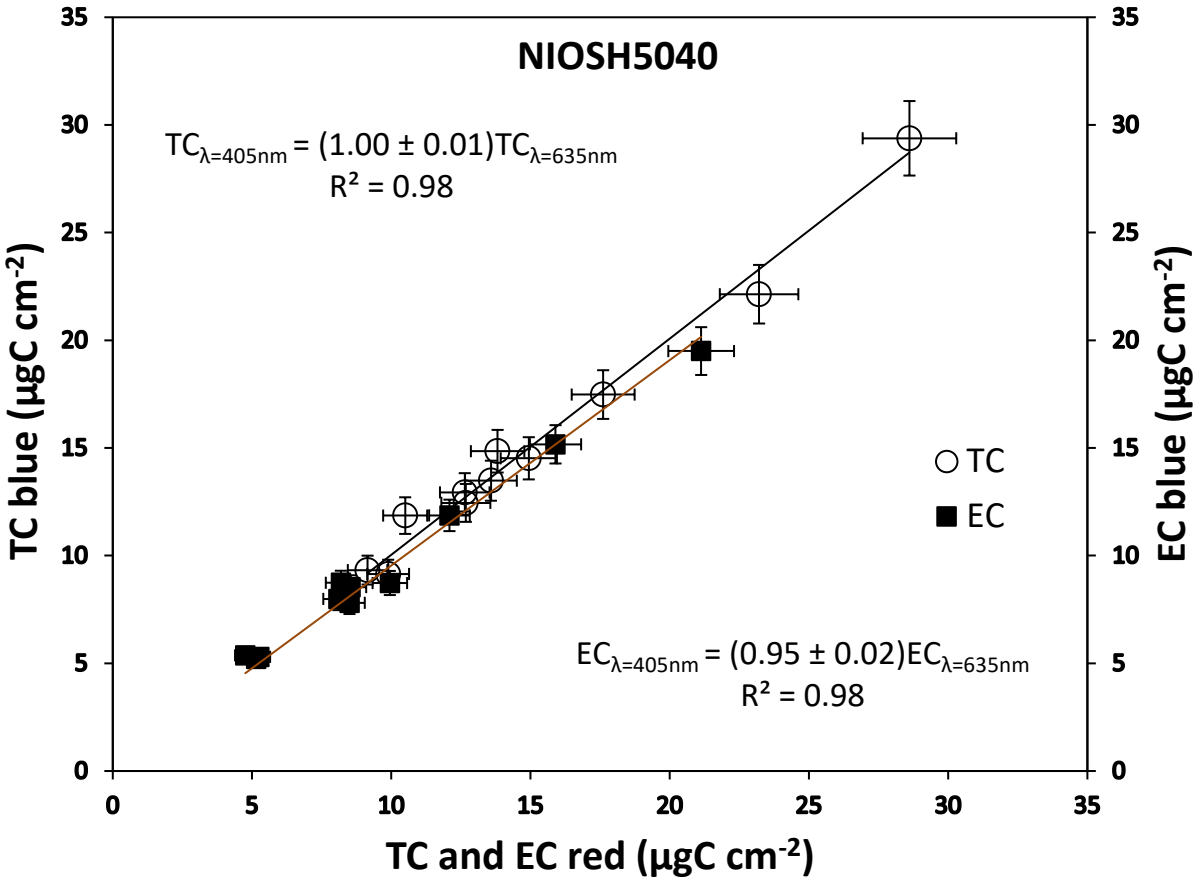

576

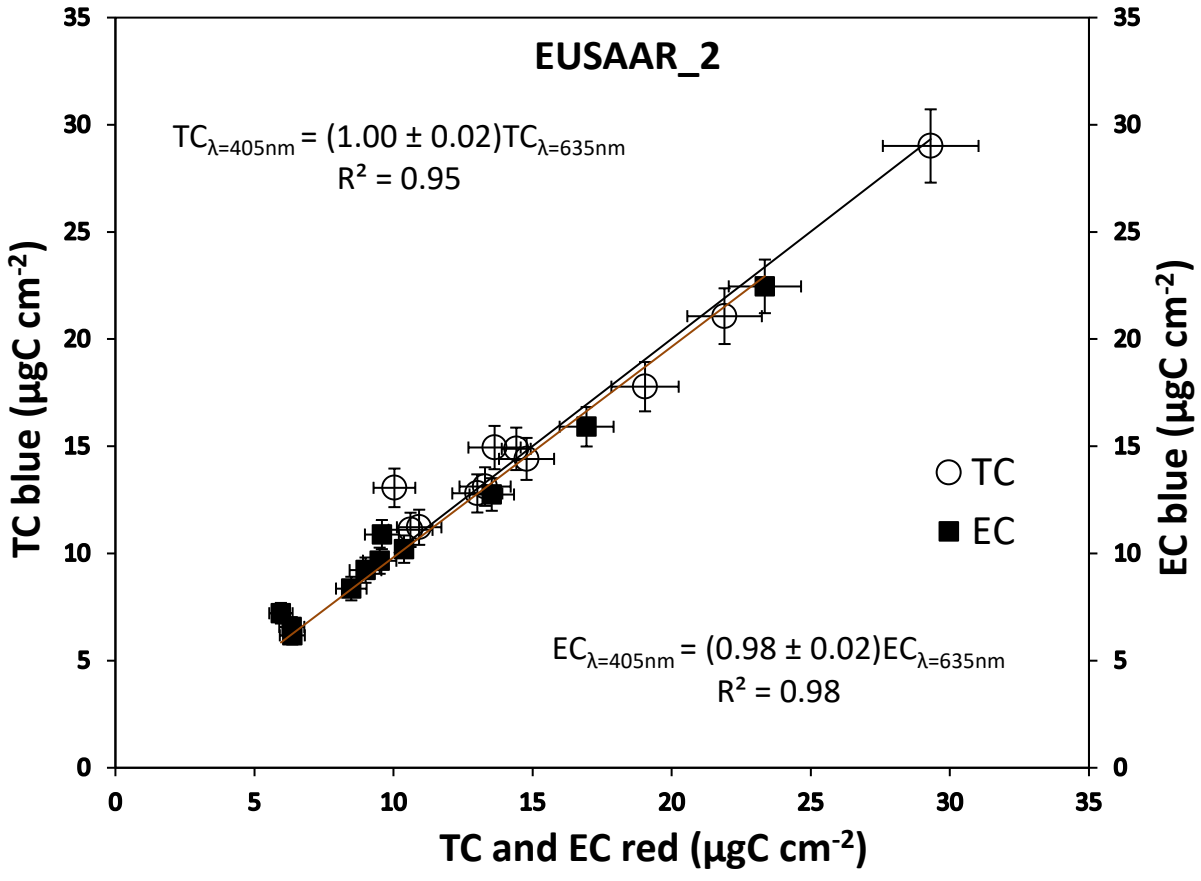

577
578 Figure 2

579

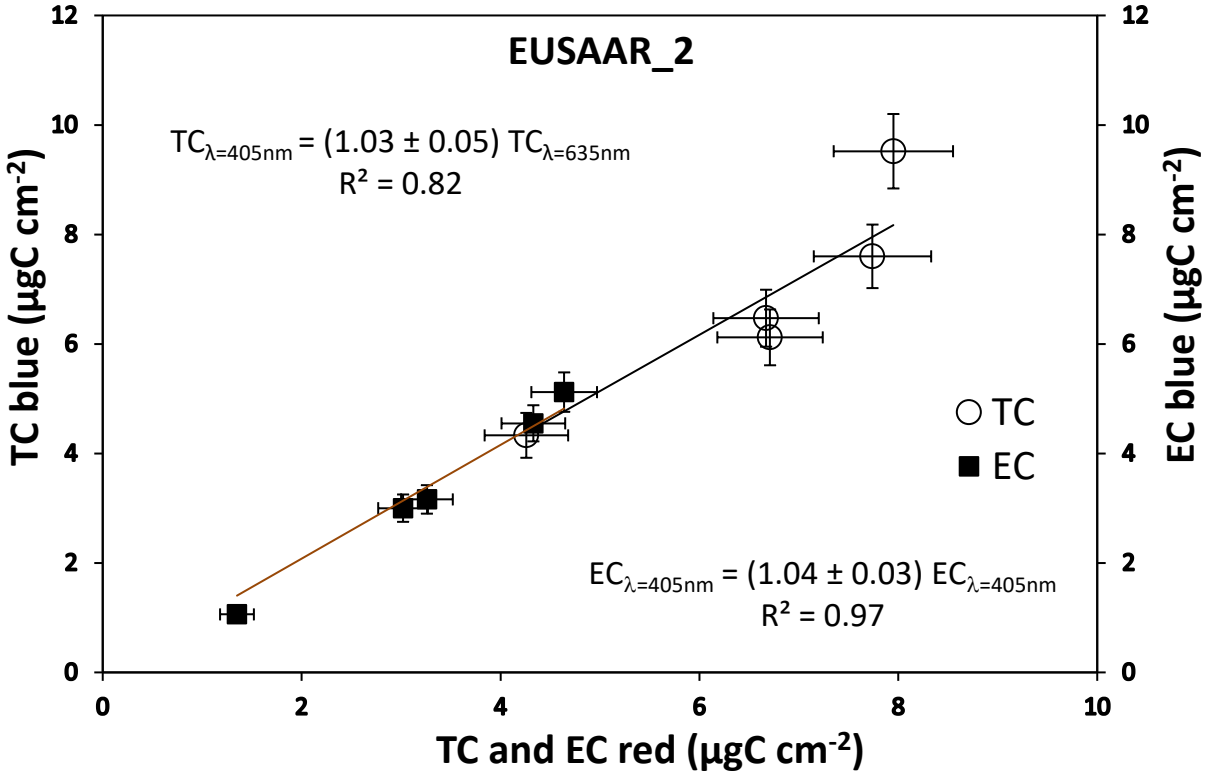

580
581 Figure 3

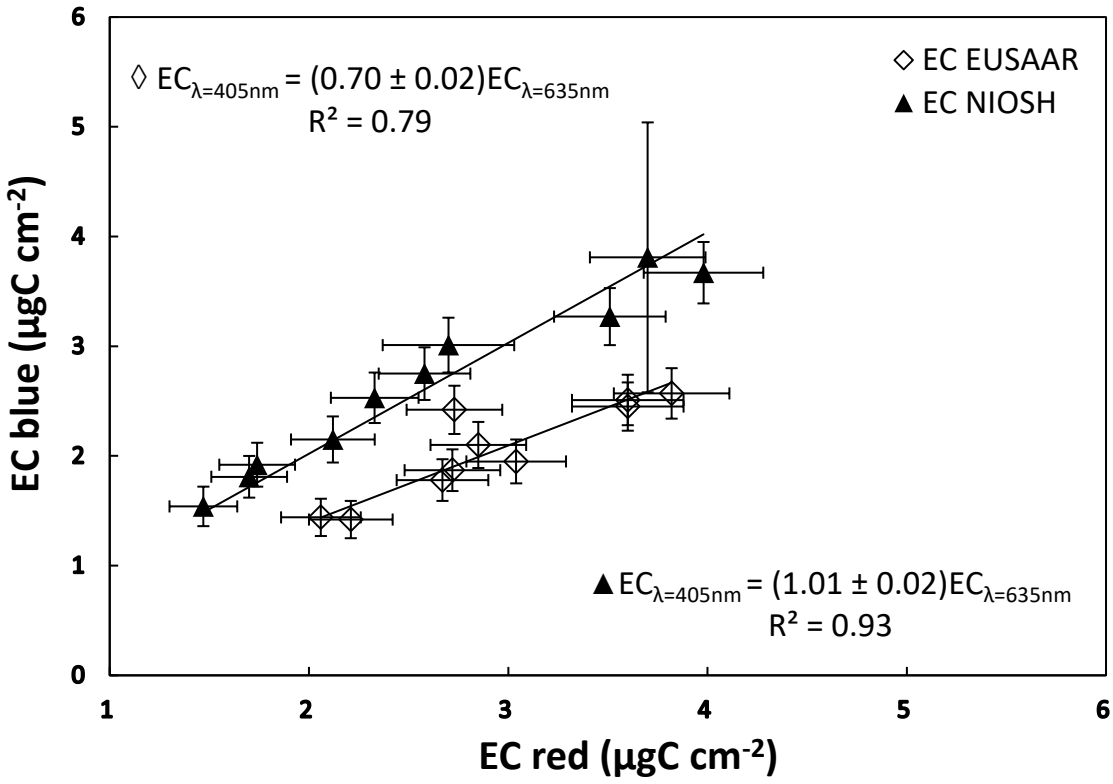

582
583 Figure 4

584

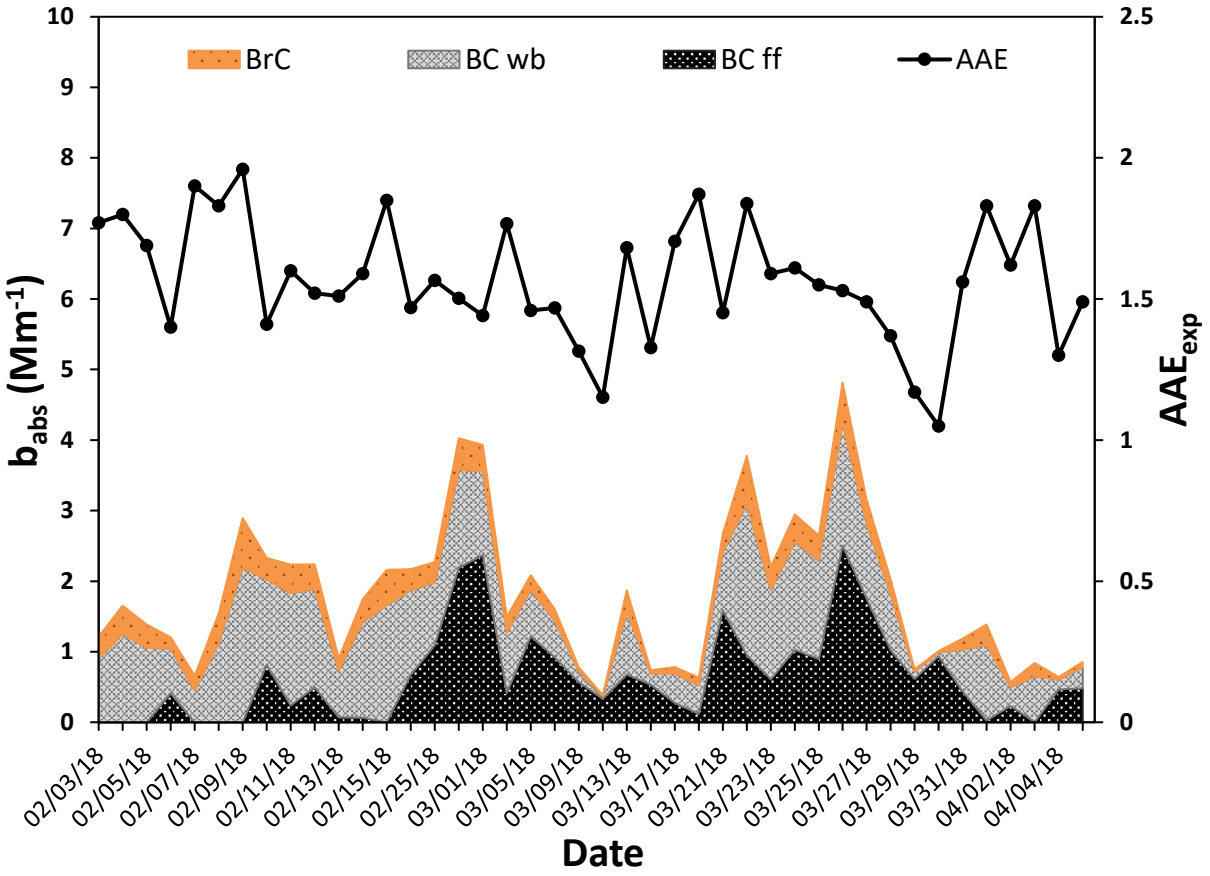

585

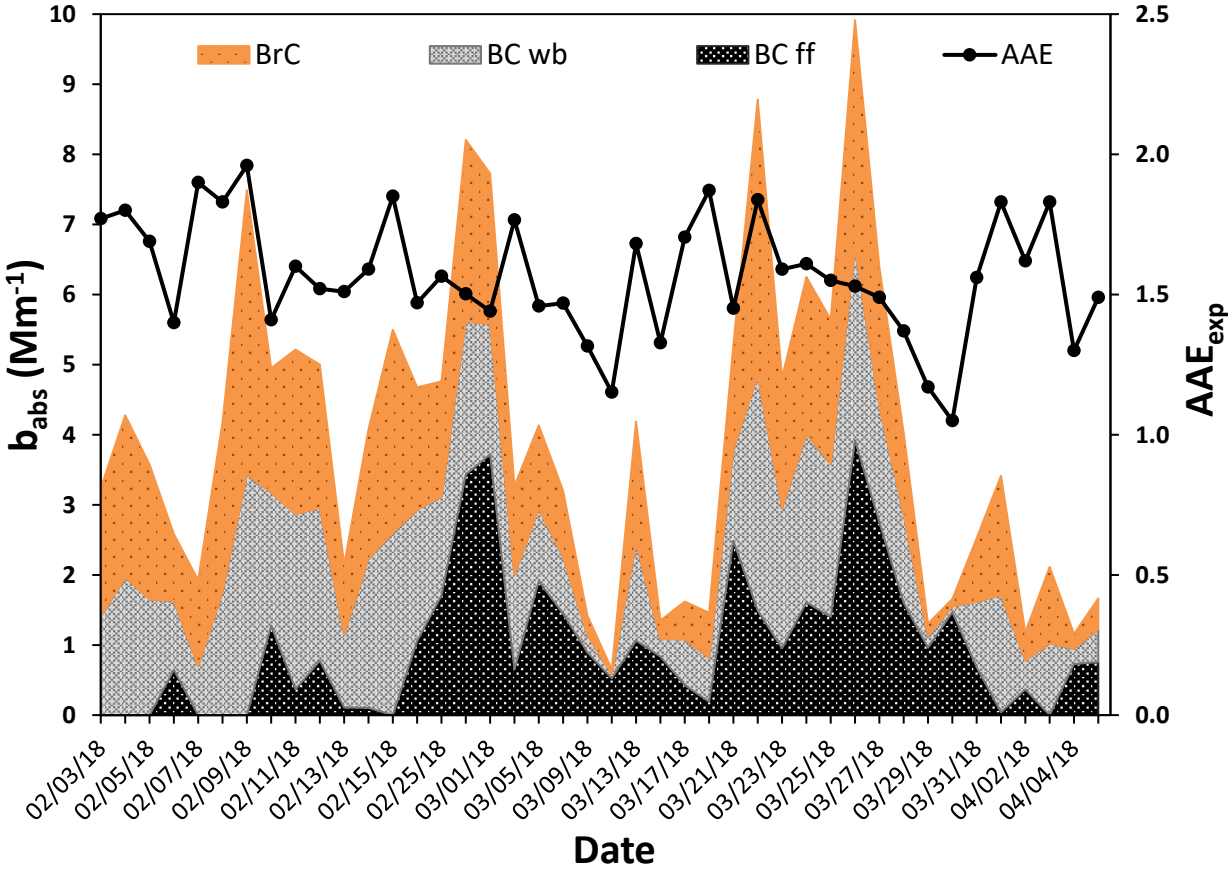

586
587 Figure 5

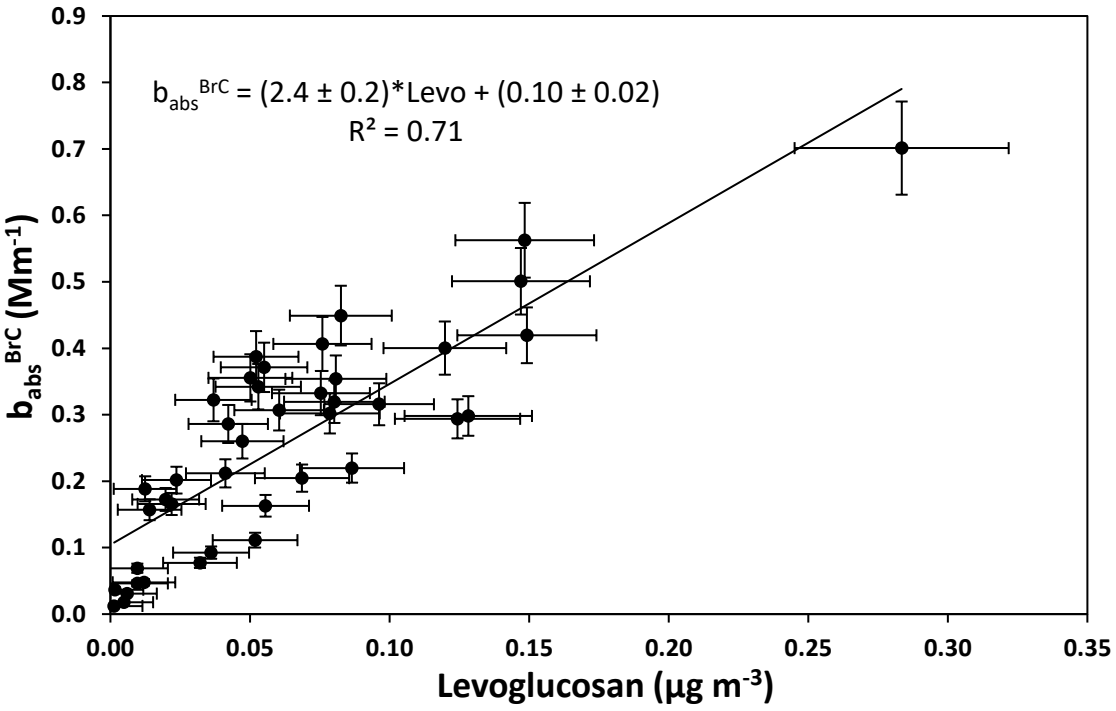

588
589
590

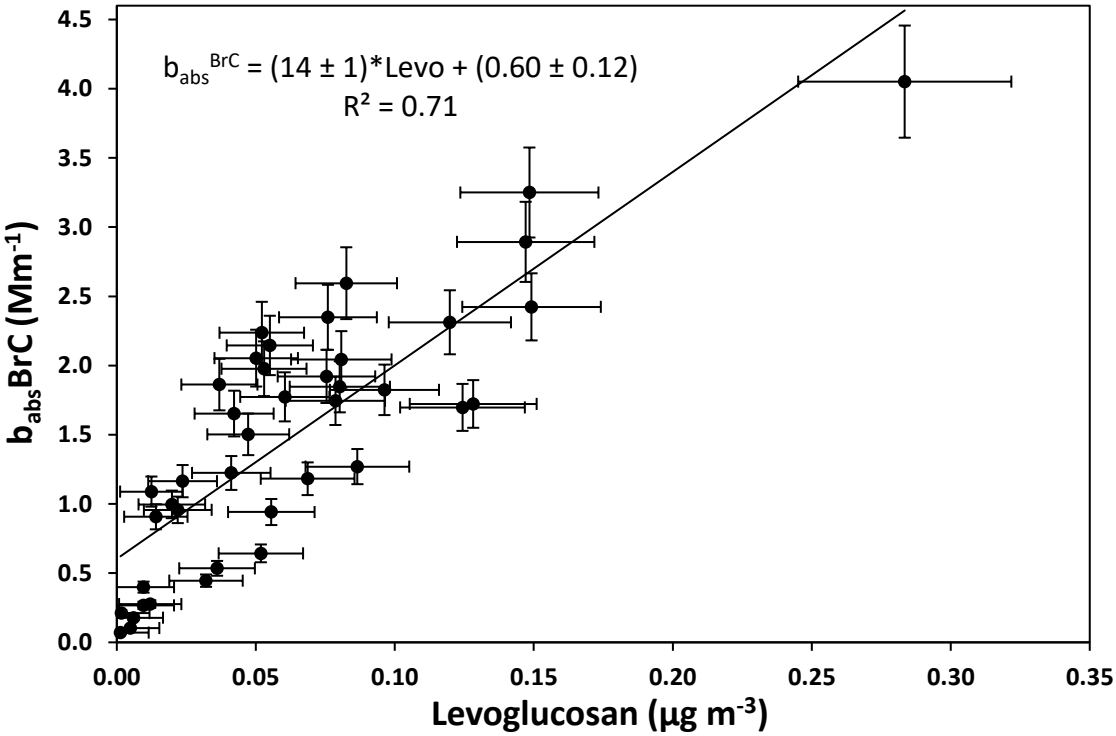

591
592 Figure 6

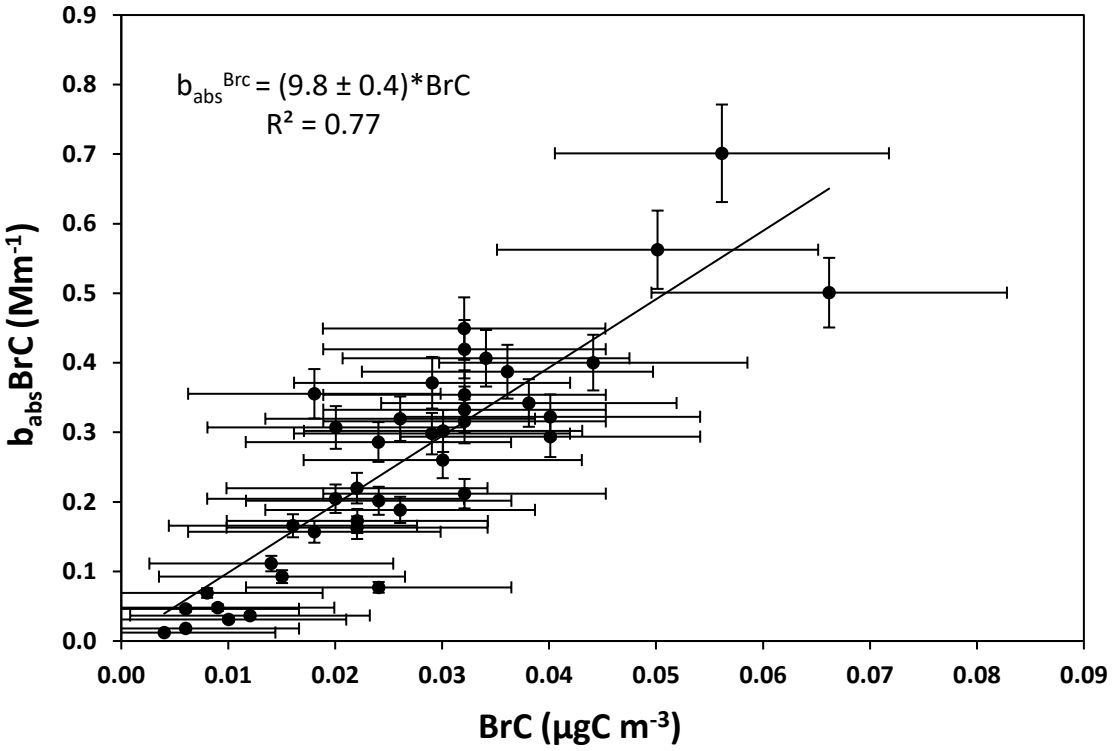

593
594

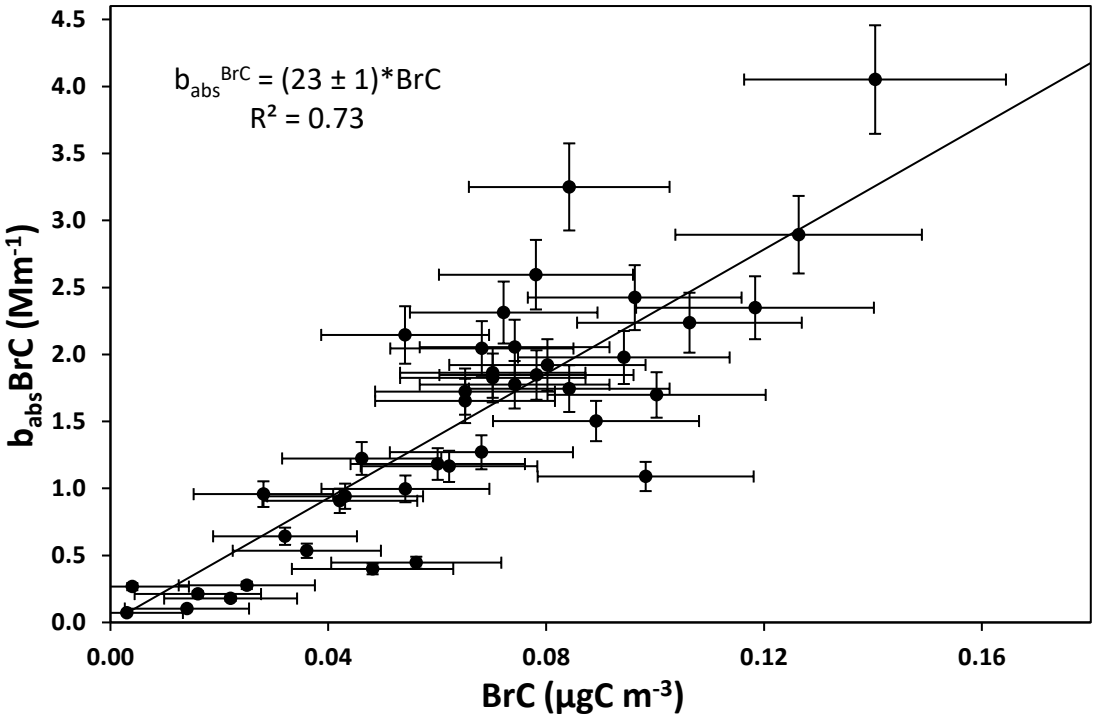

595
596 Figure 7